Adsorption of oxygen on a nickel covered $SrTiO_3$(100) surface studied by means of Auger electron spectroscopy and work function measurements

2005 J. Phys.: Condens. Matter 17 635

(http://iopscience.iop.org/0953-8984/17/4/006)

INSTITUTE OF PHYSICS PUBLISHING JOURNAL OF PHYSICS: CONDENSED MATTER

J. Phys.: Condens. Matter **17** (2005) 635–642 doi:10.1088/0953-8984/17/4/006

Adsorption of oxygen on a nickel covered $SrTiO_3(100)$ surface studied by means of Auger electron spectroscopy and work function measurements

D Vlachos[1,3], M Kamaratos[1], S D Foulias[1], Ch Argirusis[2] and G Borchardt[2]

[1] Department of Physics, University of Ioannina, 451 10 Ioannina, Greece
[2] TU Clausthal, Institut für Metallurgie, AG Thermochemie und Mikrokinetik, Robert-Koch-Straße 42, D-38678 Clausthal-Zellerfeld, Germany

E-mail: dvlachos@cc.uoi.gr

Received 17 November 2004, in final form 20 December 2004
Published 14 January 2005
Online at stacks.iop.org/JPhysCM/17/635

Abstract

The interaction of oxygen with evaporated Ni films on an Fe-doped $SrTiO_3(100)$ substrate was investigated by means of LEED, AES and work function measurements (WF) at room temperature. The adsorption of oxygen takes place on the nickel overlayer firstly by chemisorption on nickel step sites, accompanied by a reduction of the WF, and secondly on terrace sites, followed by a WF increase. After the chemisorption phase, the oxidation of the nickel overlayer starts with NiO island formation followed by bulk NiO development, which is marked by a second WF reduction. The adsorption phases of oxygen correspond closely to those of oxygen on single crystals of nickel. This indicates that the character of the Ni predeposited layers on strontium titanate seems to be metallic.

1. Introduction

The growth of metallic films on ceramics such as the perovskite-type oxide $SrTiO_3$ (STO) and $BaTiO_3$ are very important in catalysis [1, 2]. The main reason for this is that the metallic character of the adsorbate modifies the electronic properties and the chemical behaviour of the substrate. In recent years metal oxide interfaces have been intensively studied experimentally [3–9] as well as theoretically [10]. Among the metal adsorbates applied on an oxide surface, nickel is often used, mainly because of its importance as a catalyst [11, 12].

In particular, the STO(100) surface has attracted much interest, mainly in view of its technological applications as a photocatalytic electrode in photoelectrolysis [13], a substrate for the epitaxial growth of high temperature superconducting films [13, 14] and a high temperature

[3] Author to whom any correspondence should be addressed.

oxygen sensor [15–17] etc. As regards the latter, although STO is rather inert to oxygen adsorption, especially in the absence of defects, it has been shown that this oxide functions very effectively as a gas sensor, thanks to the macroscopic changes of its electrical conductivity with the ambient oxygen pressure [15, 18].

In the last decade the adsorption of different metals on the STO(100) surface has been studied to a great extent [3, 5–7, 19–24]. While most of the metals develop epitaxially on the surface [5–7], in some cases adsorbates such as Y and Ba cause reduction of the substrate, resulting in the formation of metal oxides [22, 23]. Moreover, it is believed that metal adsorbates on the STO enhance the reactivity of the surface to oxygen. Therefore, it is important to learn more about the interaction of adsorbed metals with oxygen on the STO surface, aiming at the design of novel catalysts, for industrially important reactions. One of these reactions is the production of syngas by the direct catalytic oxidation of methane [25].

In the present contribution we investigate experimentally the adsorption of oxygen on a nickel covered STO(100) surface. To this end, a STO(100) substrate, each time precovered with a different nickel quantity, was exposed to oxygen. The measurements were performed by using common surface analytical techniques, such as low energy electron diffraction (LEED), Auger electron spectroscopy (AES) and relative work function (WF) measurements.

2. Experimental details

The experiments were performed in a UHV system with the base pressure 10^{-10} mbar. The system was equipped with a four-grid LEED optics, a VG hemicylindrical electron energy analyser with energy resolution 0.3% for AES measurements, a quadrupole mass spectrometer (QMS) and an electron gun for relative WF measurements in the diode mode. The STO(100) sample was polished on one side and was doped with Fe acceptors (0.14 wt%). The sample was fixed in a tantalum case and mounted in UHV as shipped. The surface was cleaned by Ar^+ bombardment (2 keV, 1 μA) followed by heating at about 1000 K. The temperature of the specimen was measured using a Cr–Al thermocouple spot welded onto the back of the case and calibrated using an infrared pyrometer. The sample was considered clean when the carbon signal was no longer detected by AES.

Nickel was evaporated from a home-made evaporation source by passing current through a tungsten filament surrounded by Ni ribbons (99.99% purity). The nickel dosage was calibrated by means of AES measurements [26] and the coverage was measured in monolayers (ML), where 1 ML was defined to be equal to the surface atomic density of the STO substrate, $\sim 2 \times 10^{15}$ atoms cm^{-2}. Spectroscopically pure oxygen was admitted into the chamber through a leak valve. The oxygen exposure was measured in langmuirs (1 L $= 10^{-6}$ Torr s). The oxygen pressure was measured using an ion gauge.

3. Results and discussion

According to our recent results [26], nickel grows on the Fe-doped STO(100) surface in the simultaneous multilayer mode, where the layers build up at random with the nth layer starting on a fraction of the $(n-1)$th layer [27]. After we deposited Ni on the surface, we exposed the system to oxygen gas. Figure 1 shows the O(510 eV) Auger peak-to-peak height (Ap–pH) as a function of oxygen exposure on the Ni(Θ ML)/STO surface system, where $\Theta = 0.6$, 2 and 5 ML. On the Ni(0.6 ML)/STO surface, the O(510 eV) Ap–pH increases continuously up to a maximum value at an exposure of about 100 L. For higher nickel coverages, $\Theta = 2$ and 5 ML, the O(510 eV) signal increases rapidly at low exposures (<10 L), levels off in

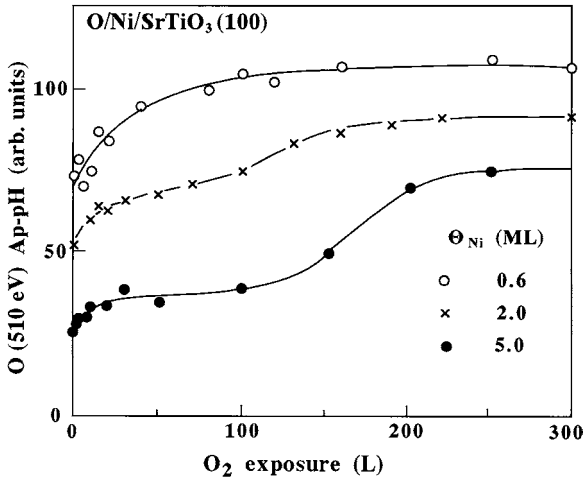

Figure 1. The O(510 eV) Ap–pH as a function of oxygen exposure on the Ni(Θ ML)/STO surface, for $\Theta = 0.6$, 2 and 5 ML.

the range of 10–50 L and then increases again up to a maximum value for exposure >200 L. We observe that the higher the nickel coverage the more distinct the plateau appearing in the O(510 eV) Auger curve. On the other hand, the Ni(61 eV) Ap–pH showed an inverse variation to that of O(510 eV), while the AES signals of Sr and Ti did not show any substantial change either of the energy and lineshape or of the intensity (not all of these signals are shown here). Apart from the 0.6 ML nickel case, the behaviours of the O and Ni AES signals are the same as those observed for oxygen exposure on Ni(110) [28–32], Ni(100) [33, 34] and Ni(111) [35] single-crystal surfaces. In all these experiments, it is generally agreed that the oxygen initially chemisorbs dissociatively on the nickel surface, while next a rapid oxidation leads to NiO island formation resulting in a final slow thickening of bulk NiO. This widely accepted model has been supported by a more recent study of the oxygen adsorption on the three low index planes of nickel, (100), (110) and (111), carried out by Stuckless *et al* [36]. More specifically, the authors, using calorimetry and sticking probability measurements, showed that the heat of oxygen adsorption drops with coverage in the chemisorption regime, indicating strong interadsorbate interactions. For the oxide formation regime, the same authors measured significantly lower heats of adsorption, while as regards the sticking probability, they observed a small increase up to a maximum and a subsequent decrease to zero when a passivating nickel oxide film, four layers thick, forms [36]. As regards our AES measurements, in the curves for 2 and 5 ML in figure 1, the initial increase of the O(510 eV) Ap–pH can be attributed to the chemisorption state of oxygen on nickel, whereas the trend of the signal to level off can be assigned to the decrease of the sticking probability at the end of the chemisorption stage [36] and the start of the oxidation stage. According to the very early model proposed by Holloway and Hudson [33, 35], the oxidation of nickel starts at nucleation points on the surface and proceeds by the lateral growth of oxide islands and final bulk oxide growth. The development of the nickel oxide islands can be related to the O(510 eV) Ap–pH increase recorded for exposures >100 L in figure 1 [30, 31, 37]. The oxide formation is verified by the Auger lineshape of the Ni(61 eV) peak (not shown), which at this stage of the oxygen adsorption looks the same as the one corresponding to the oxidation of nickel single crystals [30, 37]. This increase of oxygen uptake might be connected with an increase of the sticking probability, which has been measured for the oxidation state by Stuckless *et al* [36]. In general, the resemblance of

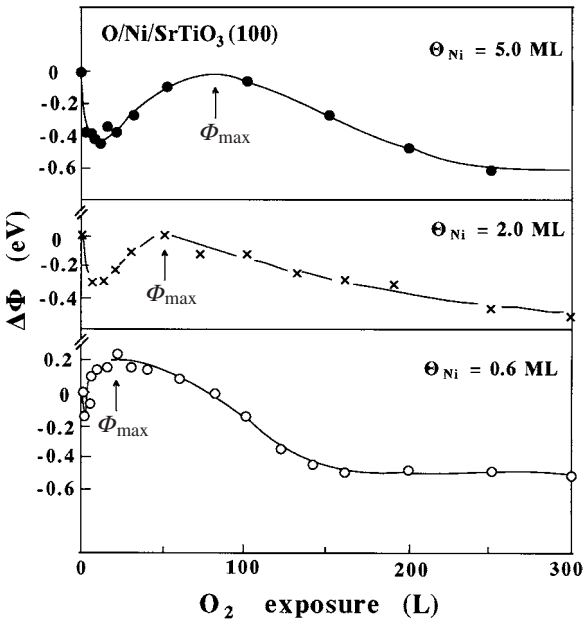

Figure 2. The WF change, $\Delta\Phi$, of the Ni(Θ ML)/STO surface versus oxygen exposure for $\Theta = 0.6$, 2 and 5 ML.

the oxygen Ap–pH variation with those previously reported leads us to the conclusion that the adsorbed nickel overlayer on STO should have an effectively metallic character. This is further supported by our recent TDS measurements, showing Ni to approach the metallic state as the coverage increases [26], and also by late photoemission measurements at the valence band of the nickel covered STO surface, where metallic Ni 3d states develop in the band gap for coverage even less than 1 ML [38]. In addition, Kido *et al* [24] have also demonstrated the metallic nature of one monolayer of nickel on STO. Going back to figure 1, it is worth pointing out the different behaviours of the 0.6 ML curve and those for 2 and 5 ML. As will be discussed below, we believe that the morphology of the nickel overlayer and possibly the interaction of the first nickel layer with the substrate account for this difference.

LEED observations showed a sharp (1×1) pattern of the clean STO(100) surface, which gradually became diffuse as the nickel coverage increased, until it disappeared at high coverages. Oxygen adsorption on the nickel covered STO surface showed no structure at room temperature.

Figure 2 shows the WF changes, $\Delta\Phi$, of the Ni(Θ ML)/STO surface with $\Theta = 0.6$, 2 and 5 ML versus oxygen exposure at RT. Initially, as the chemisorption stage starts, the WF decreases rapidly down to a minimum and then increases up to a maximum value. Finally a slow decrease follows, approaching a constant value. There are two significant observations in the $\Delta\Phi$–exposure curves as the nickel coverage becomes higher: (1) the initial WF decrease becomes more intense and (2) the maximum WF, Φ_{max}, shifts to higher oxygen exposures. It is noted that the initial decrease of WF has not been observed for oxygen adsorption on any single-crystal nickel surface [30, 32, 35, 39–42]. In order to explain qualitatively the two characteristics of the WF curves we need to mention the morphology of the Ni overlayers. According to our previous work, nickel seems to form simultaneous multilayers on STO [26], i.e. successive incomplete layers. This growth mode generates many steps and terraces. We may reasonably assume that the first chemisorbed oxygen atoms would prefer the more reactive

step sites, next to laterally less coordinated nickel atoms. If we also take into account that the radius of an O atom is roughly only half that of an Ni one, we can explain the initial decrease in WF through the creation of electrical dipoles with a vertical component, outwardly positive. This atomic configuration suggests that the initial lowering of the WF curves in figure 2 should increase with the number of step sites, which is proportional to the coverage. In fact, this seems to be true, because the initial WF decrease becomes larger with the nickel coverage. Alternatively, the initial WF decrease could be explained by oxygen atom incorporation into the Ni overlayer. However, we consider this effect unlikely, because the incorporation or surface diffusion of O atoms into single crystals of nickel at the chemisorption stage has not been reported in the literature. Furthermore, high resolution STM images obtained by Kopatzki and Behm [43] showed that the spontaneous oxygen adatom hopping rate at room temperature is very low, suggesting that diffusion across the chemisorbed layer and into the nickel surface is not probable.

The WF increase in figure 2 is attributed to O atoms occupying terrace sites. The number of adsorption sites on terraces is also proportional to the coverage, and consequently as the nickel coverage increases, more oxygen atoms are required to cover the area of the terraces. This explains reasonably well the shift of Φ_{max}, to higher oxygen exposures. However, the relaxation of the nickel atoms at terrace sites should increase the O(510 eV) Ap–pH. Instead, the oxygen signal levels off while the WF increases, at least for nickel coverage $\Theta = 2$ and 5 ML. This might be due first to the very low sticking probability of oxygen on a nickel surface, which characterizes the end of the chemisorption stage [36], and second to a tendency of the O atoms to incorporate into the Ni overlayer at the beginning of the oxidation stage. The latter should cause a reduction of the mean electric dipole moment per oxygen atom, which is probably reflected by the observed lower rate of WF increase as we approach Φ_{max} (figure 2). Indeed, in their classical papers, Holloway and Hudson [33, 35] supported an incorporation effect, as the oxidation starts at nucleation points on the surface resulting in NiO island formation. As the oxidation of the nickel overlayer advances, the oxygen uptake increases rapidly again while the WF starts decreasing, finally approaching a value which characterizes the bulk NiO. The incorporation of oxygen atoms possibly creates new surface adsorption sites, increasing the sticking probability for further bulk NiO development [36]. In general, the transition from the chemisorbed oxygen stage to the oxidation one apparently starts before Φ_{max}, while the O(510 eV) Auger signal tends to level off. This can be viewed as a surface phase transition as has been discussed by Roelofs *et al* [44]. The O(510 eV) AES curve for 0.6 ML of nickel differs from those at 2 and 5 ML, in exhibiting absence of the plateau. At this relatively low coverage, we believe that the thickness of the nickel overlayer is small (probably smaller than two atomic nickel layers). Because of this, the effect of incorporation of the O atoms into the Ni overlayer at the oxidation stage should be substantially weaker than it is at higher coverages (2 and 5 ML), with the O atoms remaining on the surface of the nickel overlayer. So the transition from the chemisorption to the oxidation stage does not show a plateau in the O(510 eV) Auger curve (figure 1). Also, at such low coverage, the majority of the Ni atoms are located next to the top surface O atoms of the substrate, promoting the Ni–O interaction. However, it is clear that this argument remains a purely qualitative interpretation and more measurements are needed with more sophisticated techniques.

Figure 3 shows the O(510 eV), Ni(848 eV), Ni(61 eV), Sr(76 eV) and Ti(380 eV) Ap–pH and the WF change, $\Delta\Phi$, of the surface system O(250 L)/Ni(5 ML)/STO(100) as a function of temperature. The O(510 eV) Ap–pH is constant up to 450 K and starts to decrease for higher temperatures, passes through a minimum at 750 K and then increases up to a maximum value. The Ni(848 eV) Ap–pH decreases also at temperatures higher than 450 K; it levels off at 750–850 K and decreases again at higher temperatures. On the other hand, the Ni(61 eV)

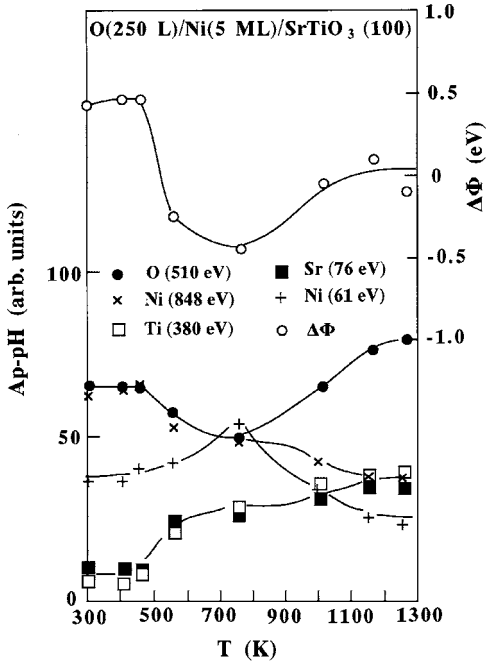

Figure 3. The O(510 eV), Ni(848 eV), Ni(61 eV), Sr(76 eV), Ti(380 eV) Ap–pH and the work function change, $\Delta\Phi$, of the O(250 L)/Ni(5 ML)/STO(100) surface system as a function of temperature.

Ap–pH increases up to 750 K and then decreases to a minimum value for temperatures higher than 1150 K. As regards the substrate elements, both the Sr(76 eV) and Ti(380 eV) Ap–pHs show gradual increase in the intensity when the temperature exceeds 450 K. All the above variations displayed in figure 3 suggest that 450 K is a critical temperature at which drastic changes occur on the surface. The decrease of the O(510 eV) Ap–pH in the range of 450–750 K can be attributed to a partial desorption of O and NiO, which actually has been verified by thermal desorption measurements (not shown). The same explanation probably accounts for the decrease of the Ni(848 eV) Ap–pH and the increase of the substrate Ap–pHs. However, the increase of the Ni(61 eV) Ap–pH is not consistent with the NiO desorption. This behaviour is probably due to the nature of the Ni $M_{2,3}VV$ Auger transition line which actually relates to a valence band transition. This line is strongly affected by the oxidation in the shape, intensity and energy as well [30, 37]. Indeed, the intensity of the Ni $M_{2,3}VV$ line of the oxidized nickel is smaller than that of the metallic Ni. So the increase of the Ni(61 eV) Ap–pH measured up to about 750 K is due to the oxygen and partial NiO desorptions (unpublished results) which take place simultaneously in this temperature range. Thus the annealing up to 750 K seems to reduce the NiO in agreement with very recent SXPS measurements [38], while some metallic Ni remains on the surface. Above 750 K the morphology of the Ni overlayers seems to change into three-dimensional particles, giving the final decrease of intensity of the Ni(61 eV) line. Finally, Ni desorption occurs at temperature >1000 K [26]. The increase of the O(510 eV) Ap–pH above 750 K can be assigned to the contribution of the substrate O atoms, which becomes stronger as the STO surface becomes less covered. In the same manner, the increase of the Ap–pH of the substrate Auger lines, Sr(76 eV) and Ti(380 eV), at temperatures above 750 K, seems to be reasonable.

Finally, $\Delta\Phi$, where $\Delta\Phi = 0$ corresponds to the WF of Ni(5 ML)/STO, is stable up to 450 K, decreases at higher temperatures, passing through a minimum at 750 K, and then increases to a value close to the initial WF. The decrease of the WF in the temperature range 450–750 K is the result of the O desorption. At even higher temperatures the WF value approaches that of the Ni(5 ML)/STO surface. Here we should point out that a significant amount of Ni, which is however much less than 5 ML, remains on the STO surface even after strong annealing [26]. This annealing probably causes changes in the stoichiometry, morphology and symmetry of the STO surface, as has been shown by recent studies [45–47]. Such changes drastically affect the final WF of the surface.

4. Conclusions

In this investigation we studied the interaction of oxygen with evaporated Ni films on the $SrTiO_3(100)$ surface at room temperature. The main techniques used were AES and WF measurements. The predeposited nickel adatoms act as active centres for the adsorption of oxygen. It seems that oxygen chemisorbs first dissociatively at the Ni step sites formed, decreasing the work function, and this process continues with chemisorption at the terrace sites, increasing the WF of the surface. When the chemisorption stage is completed, a stage of oxidation starts at nucleation points on the surface, characterized by the incorporation of the oxygen atoms into the Ni overlayer. The oxidation of the nickel results initially in the formation of NiO islands; this is followed by bulk NiO formation throughout the overlayer. The stages of adsorption of oxygen on the nickel covered STO surface are quite similar to those observed for oxygen adsorption on several single crystals of nickel. This similarity indicates that the predeposited nickel overlayer seems to be in an effectively metallic state. This work shows no evidence that the presence of Ni on the surface affects the reactivity of the STO substrate to oxygen.

Acknowledgments

D Vlachos, M Kamaratos and S D Foulias gratefully acknowledge the Hellenic State Scholarships Foundation, IKY, for the financial support of this work. Ch Argirusis and G Borchardt would like to thank the Deutsche Akademische Austauschdienst (DAAD) for partial support of this work within the IKYDA programme.

References

[1] Campell C T 1997 *Surf. Sci. Rep.* **27** 1
[2] Henry C R 1998 *Surf. Sci. Rep.* **31** 235
[3] Van Benthem K, Scheu C, Single W and Rühle M 2002 *Z. Metallk.* **93** 362
[4] Polli A D, Wagner T, Gemming T and Rühle M 2000 *Surf. Sci.* **448** 279
[5] Fu Q and Wagner T 2002 *Surf. Sci.* **505** 39
[6] Wagner T, Polli A D, Richter G and Stanzick H 2001 *Z. Metallk.* **92** 701
[7] Wagner T, Richter G and Rühle M 2001 *J. Appl. Phys.* **89** 2606
[8] Sygellou L, Zafeiratos S, Tsud N, Matolin V, Kennou S and Ladas S 2002 *Surf. Interface Anal.* **34** 545
[9] Müller D A, Shkov D A, Renedeck R, Silcoy J and Seadman D N 1998 *Phys. Rev. Lett.* **80** 4741
[10] Finnis H W 1996 *J. Phys.: Condens. Matter* **8** 5811
[11] Kordesch K and Simadar G 1996 *Fuel Cells and Their Applications* (Weinheim: VCH)
[12] Scheller G, Henne R and Borck V 1995 *J. Thermal Spray Technol.* **4** 185
[13] Henrich V E and Cox C A 1994 *The Surface Science of Metal Oxides* (Cambridge: Cambridge University Press)
[14] Chen S P 1998 *J. Mater. Res.* **13** 1848
[15] Menesklou W, Schreiner H J, Härdtl K H and Ivers-Tiffee E 1999 *Sensors Actuators* B **59** 184

[16] Zhou X, Sorensen O T, Cao Q and Xu Y 2000 *Sensors Actuators* B **65** 52
[17] Wei H, Beuermann L, Helmbold J, Borchardt G, Kempter V, Lilienkamp G and Maus-Friedrichs W 2001 *J. Eur. Ceram. Soc.* **21** 1677
[18] Lampe U, Gerbliner J and Meixner H 1992 *Sensors Actuators* B **7** 787
[19] Koslowski B, Notz R and Ziemann P 2002 *Surf. Sci.* **153** 496
[20] Conard T, Rousseau A-C, Yu L M, Ghijsen J, Sporken R, Caudano R and Johnson R L 1996 *Surf. Sci.* **359** 82
[21] Ochs T and Elsässer C 2002 *Z. Metallk.* **93** 406
[22] Andersen J E T and Møller P J 1991 *Phys. Rev.* B **44** 13645
[23] Hill D M, Meyer H M III and Weaver J H 1989 *J. Appl. Phys.* **65** 4943
[24] Kido Y, Nishimura T, Hoshino Y and Namba H 2000 *Nucl. Instrum. Methods* B **161–163** 371
[25] Hickman D A and Schmidt L D 1993 *Science* **259** 343
[26] Vlachos D, Kamaratos M, Foulias S D, Argirousis Ch and Borchardt G 2004 *Surf. Sci.* **550** 213
[27] Argile C and Rhead G E 1989 *Surf. Sci. Rep.* **10** 277
[28] Hooker M P, Grant J T and Haas T W 1976 *J. Vac. Sci. Technol.* **13** 296
[29] Rieder K H 1978 *Appl. Surf. Sci.* **2** 74
[30] Benndorf C, Egert B, Nöbl C, Seidel H and Thieme F 1980 *Surf. Sci.* **92** 636
[31] Holloway P H and Outlaw R A 1981 *Surf. Sci.* **111** 300
[32] Masuda S, Nishijima M, Sakisaka Y and Onchi M 1982 *Phys. Rev.* B **25** 863
[33] Holloway P H and Hudson J B 1974 *Surf. Sci.* **43** 123
[34] Argile C 1998 *Surf. Sci.* **409** 265
[35] Holloway P H and Hudson J B 1974 *Surf. Sci.* **43** 141
[36] Stuckless J T, Wartnaby C E, Al-Sarraf N, Dixon-Warren St J B, Kovar M and King D A 1997 *J. Chem. Phys.* **106** 2012
[37] Holloway P H and Hudson J B 1975 *J. Vac. Sci. Technol.* **12** 647
[38] Kamaratos M, Vlachos D, Foulias S D and Argirusis Ch 2004 *Surf. Rev. Lett.* **11** 1
[39] Papageorgopoulos C A and Chen J M 1975 *Surf. Sci.* **52** 40
[40] Pope T D, Bushby S J, Griffiths K and Norton P R 1991 *Surf. Sci.* **258** 101
[41] Ohtani S, Terada K and Murata Y 1974 *Phys. Rev. Lett.* **32** 415
[42] Norton P R, Bindner P E and Jackman T E 1986 *Surf. Sci.* **175** 313
[43] Kopatzki E and Behm R J 1991 *Surf. Sci.* **245** 255
[44] Roelofs L D, Einstein T L, Hunter P E, Kortan A R, Park R L and Roberts R M 1980 *J. Vac. Sci. Technol.* **17** 231
[45] Castel M R 2002 *Surf. Sci.* **505** 1
[46] Castel M R 2002 *Surf. Sci.* **516** 33
[47] Gunhold A, Beuermann L, Frerichs M, Kempter V, Gömann K, Borchardt G and Mauss-Friedrichs W 2003 *Surf. Sci.* **523** 80